HHS Public Access

Author manuscript

Angiology. Author manuscript; available in PMC 2016 April 08.

Published in final edited form as:

Angiology. 2009 ; 60(4): 441–447. doi:10.1177/0003319709335908.

Wall Shear Stress Measurement Using Phase Contrast Magnetic Resonance Imaging With Phase Contrast Magnetic Resonance Angiography in Arteriovenous Polytetrafluoroethylene Grafts

Sanjay Misra, MD, **Alex A. Fu, PhD**, **Khamal D. Misra, BS**, **James F. Glockner, MD, PhD**, and **Debabrata Mukhopadhyay, PhD**

Department of Radiology, Division of Vascular and Interventional Radiology (SM, AAF, KDM), and Department of Biochemistry and Molecular Biology (JFG, DM), Mayo Clinic College of Medicine, Rochester Minnesota

Abstract

Purpose—The purpose of the present article was to determine the changes in luminal vessel area, blood flow, and wall shear stress in both the inflow artery and the venous stenosis of arteriovenous polytetrafluoroethylene (PTFE) grafts.

Methods and materials—Polytetrafluoroethylene grafts were placed from the carotid artery to the ipsilateral jugular vein in 8 castrated juvenile male pigs. Contrast-enhanced magnetic resonance angiography (MRA) with cine phase-contrast magnetic resonance imaging (MRI) was performed 2 weeks after graft placement.

Results—The mean wall shear stress at the venous stenosis was 4 times higher than the control vein, while the inflow artery was only 2-fold higher. By day 14, venous stenosis had formed, which was characterized by narrowed area and elevated blood flow.

Conclusion—By day 14, there is venous stenosis formation in porcine arteriovenous PTFE grafts with increased shear stress with decreased area when compared to control vein.

Keywords

hemodialysis graft failure; animal models; MRI; shear stress

Introduction

There are more than 200 000 patients in the United States who have end-stage renal disease (ESRD) requiring hemodialysis.[1] Maintenance of vascular access patency is essential so that optimal delivery of hemodialysis can occur. Although the arteriovenous fistula (AVF) is the preferred vascular access, over 50% of patients with ESRD undergoing hemodialysis in the United States require polytetrafluoroethylene (PTFE) grafts for access.[1] Hemodialysis graft failure occurs because of neointimal proliferation with venous stenosis formation at the vein-

Address correspondence to: Sanjay Misra, Mayo Clinic College of Medicine, Department of Radiology, 200 First Street SW, Alfred 6460, Rochester, MN 55902; Misra.sanjay@mayo.edu.

to-graft anastomosis or proximal outflow vein.[2] A recent prospective study found primary patency (time from graft placement to the first intervention) of PTFE hemodialysis grafts to be only 23% at 1 year and 4% at 2 years.[3] To maintain graft patency, an estimated 1.22 procedures on average per year are needed: 0.54 angioplasties, 0.51 thrombectomies, and 0.17 surgical revisions. Therefore, greater than 200 000 procedures are performed annually in patients with PTFE hemodialysis grafts, resulting in more than 1 billion dollars cost per year.[3] Despite the increased morbidity associated with PTFE grafts and their rising costs, the mechanisms initiating the formation of venous stenosis remain unknown.

Multiple hemodynamic factors have been hypothesized to cause venous stenosis formation such as changes in wall shear stress,[4–9] turbulent flow,[4,10] compliance mismatch,[4,6,7] eddy currents,[7,10] or the separation of boundary layers.[10] Shear stress is the dragging force exerted on the endothelium by blood flow and causes activation of several important matrix regulatory proteins including vascular endothelial growth factor-A (VEGF-A), matrix metalloproteinases (MMPs), and others.[9,11–14] It is hypothesized that this results in adventitial and medial cellular proliferation and migration leading to neointimal thickening and venous stenosis formation.

To better understand the mechanisms responsible for hemodialysis graft failure, the porcine hemodialysis access model has been used.[8,11,15–17,18] The purpose of the present study was to investigate the vascular remodeling (wall shear stress, luminal vessel area, blood flow) changes that occur to the arteries and veins after the placement of hemodialysis PTFE grafts in pigs using magnetic resonance imaging (MRI). Luminal vessel area, wall shear stress, and blood flow changes were determined using cine phase-contrast MRI and contrast-enhanced magnetic resonance angiography (MRA). Phase-contrast MRI with MRA is a noninvasive technique that provides anatomy, flow, and velocity data simultaneously and reproducibly in a very short period of time.[19,20] This information is needed to better understand the potential mechanisms responsible for hemodialysis graft failure and thereby develop novel therapeutic interventions aimed at improving hemodialysis graft patency (Tables 1–3).

Materials and Methods

Because animals were used in the present study, approval from the Institutional Animal Care and Use Committee was obtained before any procedures were conducted. The animals were housed and handled in accordance with the guidelines of the National Institutes of Health (20). Polytetrafluoroethylene grafts (4 mm wide × 7 cm long; Gore, Flagstaff, AZ) were placed to connect either the right or the left carotid artery to the ipsilateral jugular vein in 8 castrated juvenile male pigs weighing 30 to 40 kg as described.[8,11,15–18] Sham operations were performed on the contralateral vessels to serve as controls. Before every surgical procedure, food was withheld from the pigs for 12 hours. Pigs were anesthetized intramuscularly with a combination of 5 mg/kg tiletamine hydrochloride (50 mg/mL) and zolazepam hydrochloride (50 mg/mL), 2 mg/kg xylazine (Bayer, Shawnee Mission, KS), and 0.06 mg/kg glycopyrrolate. An intravenous fluid line was placed in an ear vein for administration of 5 mg/kg zolazepam hydrochloride for induction. Pigs were intubated and placed on a positive-pressure ventilator delivering oxygen (3–5 mL/kg) and isoflurane (1%–

3%). The end-tidal CO_2 volume, oxygen saturation, heart rate, electrocardiogram, and blood pressure were monitored throughout the graft procedure.

Polytetrafluoroethylene Graft Placement

Polytetrafluoroethylene grafts were placed as described else where.[16–18] Briefly, an arteriovenous PTFE graft (4 mm diameter × 7 cm long; Gore) was placed from either the right or left carotid artery to the ipsilateral jugular vein (Figure 1A) and the contralateral vessels were isolated to serve as controls. The animals were sacrificed at 14 days (N = 8) after graft placement, and vein-to-graft anastomosis with contralateral vessels were processed for gross histological analyses. Plavix (75 mg by mouth; Bristol- Myers Squibb/ Sanofi Pharmaceuticals Partnership, Bridgewater, NJ) was started the night before and given daily until the animal was sacrificed.

Cine Phase-Contrast Magnetic Resonance Imaging and Contrast- Enhanced Magnetic Resonance Angiography

To assess hemodynamic changes and vascular remodeling of the vein-to-graft anastomosis and control vessels, MRI was performed as described previously. [16,17] Animals were anesthetized for the procedure as described previously. Magnetic resonance imaging was performed prior to sacrifice at day 14 following graft placement (Figure 1B). This was repeated 3 times for each anatomical location and the average value was used. Luminal vessel area, blood flow, and graft patency were determined using MRI. Cine phase-contrast MRI and contrast-enhanced MRA were conducted 24 hours after graft placement and prior to the animal being sacrificed. The flow, velocity, and areameasurements were obtained on the grafted vessels and on the contralateral nongrafted vessels at 20 different phases of the cardiac cycle. Using the cine phase-contrast MRI and contrast-enhanced MRA data, the following parameters were calculated: wall shear stress, Reynolds number (R_e), and luminal vessel area. All magnetic resonance (MR) examinations were performed using a Signa CVi 1.5 Tesla system (GE Medical Systems, Milwaukee, WI) with a torso-phased array coil positioned over the upper chest. After an initial 3-plane localizing scan, a test bolus of gadopentetate dimeglumine (1–2 mL) was given (Magnevist; Berlex Laboratories, Wayne, NJ), followed by a 20-mL saline flush injected at 3 mL per second. A single slice overlying the thoracic aorta was scanned repeatedly about once per second, and the time delay was noted between the injection of the contrast medium and its arrival in the aorta.

Gadolinium-enhanced 3-dimensional (3D) MRA was performed using the following scan parameters: repetition time (TR) 5 milliseconds, echo time (TE) 1.7 milliseconds, flip angle 35°, 0.75 excitations, 0.75 phase field of views (FOVs), 62.5-kHz receiver bandwidth, elliptic-centric phase-encoding, 256 × 192 scan matrix, and 20 cm × 15 cm FOV, giving an in-plane resolution of 0.78 mm × 0.78 mm. A total of 30 to 40 sections (1.2 to 1.4 mm) were obtained with 50% overlapping reconstruction in the z-direction. The scan time was 20 to 25 seconds. Contrast medium (30 mL) was injected at 3 mL per second, followed by a 20-mL saline flush at the same rate. An appropriate scan delay derived from the test bolus sequence was chosen to ensure that the acquisition of the central portion of k-space corresponded with peak arterial enhancement.

The 2-dimensional cine phase-contrast MRI sequences were conducted immediately after the 3D MRA (Figure 1B). Acquisitions were positioned perpendicular to the appropriate vessels at locations selected from maximum-intensity projection images and reformatted images from the 3D MRA as follow: (a) jugular vein 2 cm distal to the venous anastomosis (venous stenosis); (b) contralateral jugular vein (control vein); (C) carotid artery 2 cm proximal to arterial anastomosis (inflow artery); (d) contralateral carotid artery (control inflow artery); (e) carotid artery 2 cm distal to the venous anastomosis (outflow artery); (f) contralateral carotid artery (control outflow artery); (g) ascending aortic arch 2 cm proximal to the bifurcation; and (h) descending aortic arch at 2 cm distal to the bifurcation. Scan variables were TR 13.2 milliseconds, TE 4.9 milliseconds, flip angle 30°, 1 excitation, receiver bandwidth 15.6 kHz, 256 × 224 matrix, and 14-cm FOV, for an in-plane resolution of 0.55 mm × 0.62 mm. Slice thickness was 5 mm. The velocity-encoding gradient was set to 100 cm per second, unless aliasing was identified on initial acquisitions. Electrocardiogram triggering was provided by a peripheral pulse oximeter. Acquisition times generally were 20 to 30 seconds. Imaging planes (slices) were placed perpendicular to the artery or vein, with positioning guided by MRA images. Using retrospective gating and view sharing, the images were reconstructed to 20 evenly spaced time points in the cardiac cycle. Segmented k-space acquisition produced 8 views per segment. Quantitative flow information was obtained only in the direction perpendicular to the slice. All flow calculations were made on an Advantix Windows workstation (Cardiac and Flow Analysis Tools, AW Release 4.0; GE Medical Systems). This was performed by a dedicated radiologist who is fellowship trained in MRI (J.F.G.). The flow measurements were repeated 3 times within 5 mm of each other at the vein-to-graft anastomosis, and the averaged values from these 3 measurements were used. Previous work from our institution has shown that the accuracy of blood flow measurements in 5-mmdiameter vessels to be 0.6% to 4.4% for blood flow rates of 315 and 540 mL/min.[21] The intra-reviewer coefficient of variability for blood flow was low between 3 different radiologists when interpreting the images and therefore only 1 radiologist interpreted the blood flow images for the present study.[21]

Reynolds Number

At every point, where flow was laminar rather than turbulent, the R_e was calculated as $R_e = (r<v>d)/m$, where r is vessel diameter, $<v>$ is average velocity of blood, d is density of blood, and m is viscosity. Viscosity and density of blood were estimated as 0.00345 N s m^{-2} and 1000 kg/L, respectively. A R_e of less than 2000 generally indicates the lack of turbulence, [22] and at every point measured within the venous stenosis, the R_e was less than 2000. Thus, laminar flow was assumed to exist for all WSS (Wall Shear Stress) calculations.[8]

Calculation of Wall Shear Stress

The average wall shear stress throughout the cardiac cycle was determined using Poiseuille's law. For steady laminar flow in a tube, the WSS in N/m^2 may be calculated directly from the average velocity ($<v>$) in centimeters per second with the formula $WSS = 8<v>a/A$, where a is the viscosity (0.00345 N s m^{-2}) and A is the tube diameter in centimeters.[8]

Statistical Analysis

Wall shear stress and R_e were calculated for each animal from the data using phase-contrast MRI with MRA and averaged for the cardiac cycle including the values at the anastomosed vein were averaged for each animal at each time point. These values as well as luminal vessel area and flow obtained from the phase-contrast MRI with MRA were averaged for day 14 for each vessel. Values are expressed as mean ± SD.

Results

Graft Patency

All grafts were patent at 14 days. By MRI, venous stenosis formed reproducibly at the vein-to-graft anastomosis (Figure 1B).

Luminal Vessel Area

By day 14, the average area of the inflow artery was significantly higher than the control artery (33 ± 5 mm^2, 19 ± 4.9 mm^2, respectively, $P = .001$), Table 1. The average area of the venous stenosis was significantly lower than the control vein (15.1 ± 0.9 mm^2, 20.6 ± 0.9 mm^2, respectively, $P = .001$). The average area of the outflow artery was significantly lower than the control outflow artery (13.8 ± 0.4 mm^2, 22 ± 0.8 mm^2, respectively, $P = .001$). The average area of the ascending aorta remained significantly higher than the descending aorta (430 ± 78 mm^2, 239± 20 mm^2, respectively, $P = .001$). Overall, these results indicate that by day 14, early venous stenosis has formed at the vein-to-graft anastomosis.

Blood Flow Measurements

By day 14, the average blood flow of the inflow artery was significantly higher than the control artery (1122 ± 304 mL/min, 250 ± 41 mL/min, respectively, $P < .001$), Table 2. The average blood flow of the venous stenosis was significantly higher than the control vein (372 ± 81 mL/min, 124 ± 10 mL/ min, respectively, $P = .04$). The average blood flow of the outflow artery was significantly lower than the control outflow artery (103 ± 18 mL/min, 289 ± 18 mL/min, respectively, $P = .0002$). The average blood flow of the ascending aorta remained significantly higher than the descending aorta (4286 ± 757 mL/min, 2929 ± 467 mL/min, respectively, $P = .001$). Overall, these results indicate that by day 14, the shear stress at the venous stenosis has started to approach that of the inflow artery.

Wall Shear Stress

By day 14, the Reynolds number for ascending aorta, descending aorta, inflow artery, control artery, outflow artery, control outflow artery, venous stenosis, and control vein was less than 1000, and therefore we assumed that there was lack of turbulent blood flow. By day 14, the average shear stress of the inflow artery was significantly higher than the control artery (2.5 ± 0.8 N/m^2, 1.3± 0.6 N/m^2, respectively, $P = .02$), Table 3. The average shear stress of the venous stenosis was significantly higher than the control vein (2.6 ± 0.5 N/m^2, 0.6 ± 0.07 N/m^2, respectively, $P = .001$). The average shear stress of the outflow artery was significantly lower than the control outflow artery (0.9 ± 0.01 N/m^2, 1.6 ± 0.2 N/m^2, respectively, $P = .05$). The average shear stress of the ascending aorta remained significantly

higher than the descending aorta (0.2 ± 0.08 N/m^2, 0.3 ± 0.09 N/m^2, respectively, P = .001). Overall, these results indicate that by day 14, the shear stress at the venous stenosis is significantly higher than the control vein almost 4-fold. Meanwhile, at the inflow artery, the shear stress is significantly higher than the control artery, almost 2-fold.

Discussion

On a cellular level, hemodialysis PTFE graft failure is caused by adventitial and medial cellular proliferation and migration resulting in thickened media and neointima resulting in venous stenosis formation.[23] Many different factors have been hypothesized to cause venous stenosis formation, including changes in wall shear stress with elaboration of several important matrix regulatory proteins including MMPs, VEGF-A, and others resulting in cellular proliferation and migration causing neointimal formation and venous stenosis formation.[23] Therefore, understanding the changes in wall shear stress is important as it could provide insight into the pathophysiology of hemodialysis graft failure.

In the current study, we determined the changes in wall shear stress, blood flow, and luminal vessel area in anastomosed arteries and veins following placement of PTFE grafts using cine phase-contrast MRI with MRA. Following the placement of PTFE grafts, anastomosed arteries and veins respond to increased blood flow differently with respect to wall shear stress, luminal vessel area change, and blood flow. This is consistent with previous studies that have investigated the changes in mean luminal vessel area increases and the mean wall shear stress decreases and in the aorta and anastomosed artery supplying the PTFE grafts.[23–26] However, in the anastomosed vein, the mean luminal vessel area decreases and the mean wall shear stress and mean intima to media ratio increased over time.[9,27]

There have been many previous studies using ultrasound with arteriovenous PTFE hemodialysis grafts.[4,28] In the current study, we used MRI with MRA because it has several advantages over ultrasound. First, it can provide both anatomic data (angiogram) and physiologic flow data reproducibly in a relatively short period of time.[10,29,30] Second, it allows for flow and velocity measurements to be obtained throughout the cardiac cycle, which can be used to estimate the wall shear stress and wall shear stress rate; both of which are felt to be important in stenosis and atherosclerotic plaque formation.[10,29,30] Finally, MRI is not limited to evaluating superficial structures as is ultrasound. The MRI data can be used with computational fluid dynamic modeling to determine in vivo wall shear stresses.[10,29–31]

The results from the current study are in agreement with previous studies using ultrasound or MRI arteriovenous hemodialysis grafts used to estimate wall shear stress.[10,29–31] Using dogs, Fillinger et al[28] placed bilateral 6-mm diameter PTFE loop grafts were placed to connect the femoral artery to femoral vein in dogs with 1 side being banded to reduce blood flow by 50% and the other side being unbanded and the normal diameter.[28] In these experiments, Fillinger et al showed that there was increased turbulence at the anastomosed vein with R_e number in the range of 500 to 1000. Furthermore, a correlation between increased turbulence and thickness of the intima and media at the anastomosed vein was identified, which was observed in unbanded grafts when compared to banded grafts.[4] As expected, unbanded grafts had higher blood flow and blood velocity measurements when

compared to the banded grafts. Similar findings were observed in a separate study with tapered grafts in which 4- to 7-mm taper grafts had decreased venous anastomotic narrowing when compared to 7- to 4-mm taper grafts and 6-mm straight grafts.[4]

Recently, a study was performed in pigs in which straight 4-mm × 2-cm PTFE grafts were placed to connect the iliac artery to iliac vein.[9,11,32–34] By day 14, the mean wall shear stress at the venous stenosis was significantly elevated at 2.5 N/m^2 when compared to the control vein (0.6 N/m^2). The inflow artery supplying the graft had a mean wall shear stress of 1.5 N/m^2 while the control artery was 0.6 N/m^2. More recently, there was a study performed in pigs with renal insufficiency and arteriovenous PTFE grafts placed to connect the carotid artery to jugular vein.[9,11,32–34] In this study, the investigators observed that the mean WSS at the vein-to-graft anastomosis had a bimodal peak. The mean WSS was 7.3 ± 2.1 N/m^2 by day 1, decreased to 5.1± 1.8 N/m^2 by day 3, subsequently peaked at 8.8± 1.6 N/m^2 by day 7 ($P < .05$, compared to days 3 and 14) and was 4.3 ± 0.5 N/m^2 by day 14. These 2 studies are in agreement with our present work. In the current study, we observed significantly increased shear stress 2.6 N/m^2 when compared to the control veins. Similarly, the shear stress of the inflow artery was 2.5 N/m^2 when compared to control artery. However, the shear stress in the control vein was half of that of the control artery.

There are several limitations that need to be discussed. The major limitation of the current study is that mean wall shear stress was calculated with the law of Poiseuille, which assumes that the vessels are circular. For most arteries, this is a reasonable assumption, but it does not hold true for veins as they are elliptical. In addition, this law assumes that there is steady laminar flow within a uniformly shaped tubular structure, which is not entirely true, particularly within venous stenosis where local turbulent flow may occur. Visually, turbulent flow was observed at the venous stenosis during the phase-contrast MRI measurements. Future experiments are being planned to determine time-dependent changes in the grafted vessels as well as using the MRI data and combining it with computational fluid dynamic modeling.

Arteries supplying hemodialysis grafts and outflow veins respond to the increased blood flow differently. At the venous anastomosis, high blood flow results in increase mean wall shear stress and decreased mean luminal vessel area. The decrease in the mean area results from neointimal hyperplasia, which may be caused by increased shear stress that activates matrix regulatory proteins leading to neointimal hyperplasia.[9,11,32–34] Understanding the interaction between shear stress and these proteins will help provide insight into the pathophysiology of hemodialysis graft failure, thereby improving outcomes in patients.

References

1. Schwab SJ, Harrington JT, Singh A, et al. Vascular access for hemodialysis. Kidney Int. 1999; 55(5):2078–2090. [PubMed: 10231476]
2. Rekhter M, Nicholls S, Ferguson M, Gordon D. Cell proliferation in human arteriovenous fistulas used for hemodialysis. Arterioscler Thromb. 1993; 13(4):609–617. [PubMed: 8096766]
3. Miller PE, Carlton D, Deierhoi MH, Redden DT, Allon M. Natural history of arteriovenous grafts in hemodialysis patients. Am J Kidney Dis. 2000; 36(1):68–74. [PubMed: 10873874]

4. Fillinger M, Reinitz ER, Schwartz RA, et al. Graft geometry and venous intimal-medial hyperplasia in arteriovenous loop grafts. J Vasc Surg. 1990; 11(4):556–566. [PubMed: 2182916]
5. Hofstra L, Bergmans DC, Hoeks AP, Kitslaar PJ, Leunissen KM, Tordoir JH. Mismatch in elastic properties around anastomoses of interposition grafts for hemodialysis access. J Am Soc Nephrol. 1994; 5(5):1243–1250. [PubMed: 7873735]
6. Hofstra L, Bergmans DC, Leunissen KM, et al. Anastomotic intimal hyperplasia in prosthetic arteriovenous fistulas for hemodialysis is associated with initial high flow velocity and not with mismatch in elastic properties. J Am Soc Nephrol. 1995; 6(6):1625–1633. [PubMed: 8749690]
7. Shu MC, Noon GP, Hwang NH. Phasic flow patterns at a hemodialysis venous anastomosis. Biorheology. 1987; 24(6):711–722. [PubMed: 3502767]
8. Misra S, Woodrum DA, Homburger J, et al. Assessment of wall shear stress changes in arteries and veins of arteriovenous polytetrafluoroethylene grafts using magnetic resonance imaging. Cardiovasc Intervent Radiol. 2006; 29:624–629. [PubMed: 16729233]
9. Misra S, Fu AA, Puggioni A, et al. Increased shear stress with up regulation of VEGF-A and its receptors and MMP-2, MMP-9, and TIMP-1 in venous stenosis of hemodialysis grafts. Am J Physiol Heart Circ Physiol. 2008; 294(5):H2219–H2230. [PubMed: 18326810]
10. Longest PW, Kleinstreuer C, Andreotti PJ. Computational analyses and design improvements of graft-to-vein anastomoses. Crit Rev Biomed Eng. 2000; 28(1–2):141–147. [PubMed: 10999378]
11. Misra S, Doherty MG, Woodrum D, et al. Adventitial remodeling with increased matrix metalloproteinase-2 activity in a porcine arteriovenous polytetrafluoroethylene grafts. Kidney Int. 2005; 68(6):2890–2900. [PubMed: 16316367]
12. Misra S, Fu AA, Anderson JL, et al. The rat femoral arteriovenous fistula model: Increased expression of MMP-2 and MMP-9 at the venous stenosis. J Vasc Interv Radiol. 2008; 19(4):587–594. [PubMed: 18375305]
13. Misra S, Fu AA, Rajan DK, et al. Expression of hypoxia inducible factor-1 alpha, macrophage migration inhibition factor, matrix metalloproteinase-2 and -9, and their inhibitors in hemodialysis grafts and arteriovenous fistulas. J Vasc Interv Radiol. 2008; 19(2):252–259. [PubMed: 18341958]
14. Roy-Chaudhury P, Kelly BS, Miller MA, et al. Venous neointimal hyperplasia in polytetrafluoroethylene dialysis grafts. Kidney Int. 2001; 59(6):2325–2334. [PubMed: 11380837]
15. Johnson MS, McLennan G, Lalka SG, Whitfield RM, Dreesen RG. The porcine hemodialysis access model. J Vasc Interv Radiol. 2001; 12(8):969–977. [PubMed: 11487678]
16. Misra S, Fu AA, Puggioni A, et al. Increased expression of Hypoxia inducible factor-1a in a porcine model of chronic renal insufficiency with arteriovenous polytetrafluoroethylene grafts. J Vasc Interv Radiol. 2008; 19(2):260–265. [PubMed: 18341959]
17. Misra S, Fu AA, Anderson JL, et al. Fetuin-A expression in early venous stenosis formation in a porcine model of hemodialysis graft failure. J Vasc Interv Radiol. 2008; 19(10):1477–1482. [PubMed: 18693047]
18. Hughes D, Fu AA, Puggioni A, et al. Adventitial transplantation of blood outgrowth endothelial cells in porcine haemodialysis grafts alleviates hypoxia and decreases neointimal proliferation through a matrix metalloproteinase-9-mediated pathway—a pilot study. Nephrol Dial Transplant. 2009; 24(1):85–96. [PubMed: 18786975]
19. Pelc NJ, Herfkens RJ, Shimakawa A, Enzmann DR. Phase contrast cine magnetic resonance imaging. Magn Reson Q. 1991; 7(4):229–254. [PubMed: 1790111]
20. Pelc NJ, Sommer FG, Li KC, Brosnan TJ, Herfkens RJ, Enzmann DR. Quantitative magnetic resonance flow imaging. Magn Reson Q. 1994; 10(3):125–147. [PubMed: 7811608]
21. King BF, Torres VE, Brummer ME, et al. Magnetic resonance measurements of renal blood flow as a marker of disease severity in autosomal-dominant polycystic kidney disease1. Kidney Int. 2003; 64(6):2214–2221. [PubMed: 14633145]
22. Yellin E. Laminar-turbulent transition process in pulsatile flow. Circ Res. 1966; 19(4):791–804. [PubMed: 5917851]
23. Langille BL, Bendeck MP, Keeley FW. Adaptations of carotid arteries of young and mature rabbits to reduced carotid blood flow. Am J Physiol. 1989; 256(4 pt 2):H931–H939. [PubMed: 2705563]
24. Kamiya A, Togawa T. Adaptive regulation of wall shear stress to flow change in the canine carotid artery. Am J Physiol. 1980; 239(1):H14–H21. [PubMed: 7396013]

25. Miller VM, Aarhus LL, Vanhoutte PM. Modulation of endothelium-dependent responses by chronic alterations of blood flow. Am J Physiol. 1986; 251(3 pt 2):H520–H527. [PubMed: 3752266]

26. Zarins CK, Zatina MA, Giddens DP, Ku DN, Glagov S. Shear stress regulation of artery lumen diameter in experimental atherogenesis. J Vasc Surg. 1987; 5(3):413–420. [PubMed: 3509594]

27. Rotmans JI, Velema E, Verhagen HJ, et al. Rapid, arteriovenous graft failure due to intimal hyperplasia: a porcine, bilateral, carotid arteriovenous graft model. J Surg Res. 2003; 113(1):161–171. [PubMed: 12943826]

28. Fillinger M, Reinitz ER, Schwartz RA, et al. Beneficial effects of banding on venous intimal-medial hyperplasia in arteriovenous loop grafts. Am J Surg. 1989; 158(2):87–94. [PubMed: 2757149]

29. Kohler U, Marshall I, Robertson MB, Long Q, Xu XY, Hoskins PR. MRI measurement of wall shear stress vectors in bifurcation models and comparison with CFD predictions. J Magn Reson Imaging. 2001; 14(5):563–573. [PubMed: 11747008]

30. Wu SP, Ringgaard S, Oyre S, Hansen MS, Rasmus S, Pedersen EM. Wall shear rates differ between the normal carotid, femoral, and brachial arteries: an in vivo MRI study. J Magn Reson Imaging. 2004; 19(2):188–193. [PubMed: 14745752]

31. Long Q, Xu XY, Collins MW, Griffith TM, Bourne M. The combination of magnetic resonance angiography and computational fluid dynamics: a critical review. Crit Rev Biomed Eng. 1998; 26(4):227–274. [PubMed: 10065891]

32. Shi Y, Patel S, Niculescu R, Chung W, Desrochers P, Zalewski A. Role ofmatrixmetalloproteinases and their tissue inhibitors in the regulation of coronary cell migration. Arterioscler Thromb Vasc Biol. 1999; 19(5):1150–1155. [PubMed: 10323763]

33. Southgate KM, Mehta D, Izzat MB, Newby AC, Angelini GD. Increased secretion of basement membrane- degrading metalloproteinases in pig saphenous vein into carotid artery interposition grafts. Arterioscler Thromb Vasc Biol. 1999; 19(7):1640–1649. [PubMed: 10397681]

34. Zempo N, Kenagy RD, Au YP, et al. Matrix metalloproteinases of vascularwall cells are increased in balloon-injured rat carotid artery. J Vasc Surg. 1994; 20(2):209–217. [PubMed: 8040944]

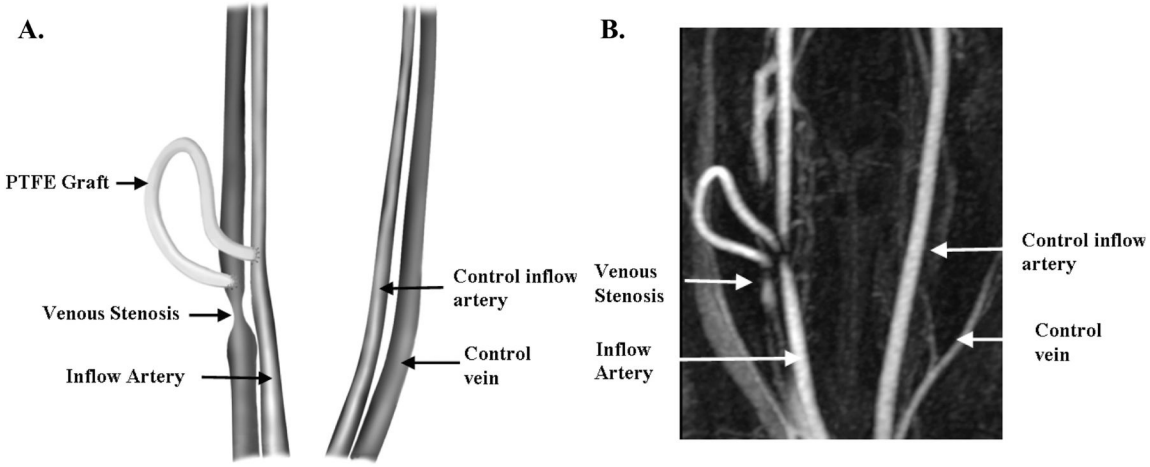

Figure 1.
Schematic representation of arteriovenous fistula creation (A) with representative MRI (B).

Table 1

Average Luminal Vessel Area at Day 14 (mm^2)

	Day 14
Inflow artery	33 ± 5
Control artery	19.1 ± 4.9
Venous stenosis	15.1 ± 0.9
Control vein	20.6 ± 0.9
Outflow artery	13.8 ± 0.4
Control outflow artery	22 ± 0.8
Ascending aorta	430 ± 76
Descending aorta	239 ± 20

Table 2

Average Blood Flow Measurements at Day 14 (mL/min)

	Day 14
Inflow artery	1122 ± 304
Control artery	250 ± 41
Venous stenosis	307 ± 70
Control vein	124 ± 10
Outflow artery	103 ± 18
Control outflow artery	289 ± 18
Ascending aorta	4286 ± 757
Descending aorta	2929 ± 467

Table 3

Average Wall Shear Stress (N/m^2) at Day 14 (D14)

	Day 14
Inflow artery	2.5 ± 0.8
Control artery	1.3 ± 0.6
Venous stenosis	2.6 ± 0.5
Control vein	0.6 ± 0.07
Outflow artery	0.8 ± 0.01
Control outflow artery	1.6 ± 0.2
Ascending aorta	0.2 ± 0.08
Descending aorta	0.3 ± 0.09